Available online at www.sciencedirect.com
SCIENCE DIRECT®
Antiviral Research 62 (2004) 65–71
Antiviral Research
www.elsevier.com/locate/antiviral

Synthesis, characterization and antiviral activity against influenza virus of a series of novel manganese-substituted rare earth borotungstates heteropolyoxometalates

Jie Liu [a,*], Wen-Jie Mei [b], An-Wu Xu [a], Cai-Ping Tan [a], Shuo Shi [a], Liang-Nian Ji [a]

[a] *Department of Chemistry, The Key Laboratory of Gene Engineering of Education Ministry, Zhongshan University, Guangzhou 510275, PR China*
[b] *Department of Pharmaceutical, Guangdong Pharmaceutical University, Guangzhou 510315, PR China*

Received 23 September 2003; accepted 10 December 2003

Abstract

A series of novel manganese-substituted mixed-valence rare earth borotungsto-heteropoly blues, $Ln_2H_3[BW_9{}^{VI}W_2{}^{V}Mn(H_2O)O_{39}]\cdot 12H_2O$ (Ln(2), Ln = La, Ce, Pr, Nd, Sm, Eu and Gd), as well as their corresponding heteropoly acids (Ln(0)), have been prepared and characterized by cyclic voltammetry (CV), infrared (IR), ultraviolet (UV), thermal gravimetric (TG) and differential thermal (DTA) analysis, X-ray photoelectron spectroscopy (XPS) and electrochemistry. It's shown that the heteropoly blues anion in Ln(2) still retains the α-Keggin structure but with a slight distortion as heteropoly acids do, and Mn and W atoms distribute statistically in the whole molecular. At the same time, the cell toxicity and antiviral activity of these rare earth borotungstateheteropoly blues against influenza virus type A and type B in MDCK cells have been investigated using plaque reduction assay. The results elucidated that these complexes exhibit a significantly inhibitory activity and almost no cytotoxicity comparable with those obtained from virazole, and the anti-virus activity depend on the structure of these complexes.
© 2004 Elsevier B.V. All rights reserved.

Keywords: Rare earth borotungstoheteropoly blues; Influenza virus; Antiviral activity

1. Introduction

In this year, controlling of human influenza virus infections continues to be a major public health goal. The antiviral drugs now available for prophylaxis influenza, such as amantadine and rimantadine, are ineffective against influenza B virus infections (Wilson et al., 1980; Heider et al., 1981; Mori et al., 1995; Moskovitz, 1988), and their utilization in clinic is further limited by the rapid emergence of resistant virus mutants (Wray et al., 1985, 1986; Wyde et al., 1986; Mori et al., 1996). Due to the rapid changes occurring in the antigenic of influenza virus, vaccine efficacy is also curtailed. Relenza and GS4071 were reported to be potent inhibitor of influenza A and B viral neuraminidases (Burger et al., 2000; Colman, 2002; McKimm-Breschkin, 2000; Sidwell et al., 1998), but they were expensive and their efficiency in the long run is still remain to be seen.

The broad-spectrum antiviral activity of heteropoly complexes has been reported (Busserearu et al., 1988; George et al., 1990; Ikeda et al., 1993; Shigeta et al., 1995a,b; Ni and Boudinot, 1995; Yamase et al., 1996; Ni et al., 1994). Some of these complexes exhibit excellent inhibitory activities against many viruses (Bardos et al., 1992; Kim et al., 1994; Jeffrey et al., 1998; Liu et al., 2000), and some others have even shown RNA and DNA virus-inhibitory activity (Shigeta et al., 1995a; Tomita et al., 1989; Fukuma et al., 1991; Inouye et al., 1991, 1993; Hill et al., 1990). Heteropoly complexes with Keggin-type structures have also been reported as inhibitors of arenaviruses (Yamamoto et al., 1992), human immunodeficiency virus HIV-1, HIV-2 (Bardos et al., 1992; Pauwele et al., 1988; Yamamoto et al., 1992; Inouye et al., 1990, 1992; Take et al., 1991; Weeks et al., 1992) and other retroviruses (Yamamoto et al., 1992), HCMV (Ikeda et al., 1993), herpes simplex virus (HSV types 1 and 2; Fukuma et al., 1991), thymidine kinase deficient herpes simplex virus (Ikeda et al., 1993), influenza viruses (Barnard et al., 1997; Huffman et al., 1997; Liu et al., 2001; Mori et al., 1996; Shigeta et al., 1995b), measles virus (Shigeta et al., 1995b), parainfluenza virus (Shigeta et al., 1995b), rhabdovirus (Yamamoto et al., 1992), RSV (Ikeda et al., 1993) and togaviruses (Yamamoto et al., 1992). More recently, Ikeda et al. reported the antiviral activity of

* Corresponding author. Tel.: +86-20-8403-4540; fax: +86-20-8403-5497.
E-mail address: cesliuj@zsu.edu.cn (J. Liu).

0166-3542/$ – see front matter © 2004 Elsevier B.V. All rights reserved.
doi:10.1016/j.antiviral.2003.12.004

PM-19 ($K_7[PTi_2W_{10}O_{40}]\cdot 6H_2O$) in ddY mice, and the results indicated that the complex can prevent the death of mice infected with HSV-1 and HSV-2 effectively (Ikeda et al., 1993; Dan et al., 2002). However, heteropolymetalates, which are unstable at the physiological pH value, only exhibit short-lived effects. One method to resolve the problem is to reduce heteropolymetalates to heteropoly blues (Liu et al., 1998a,b, 2000). Heteropoly blues, usually containing W (VI) and W (V), Mo (VI) and Mo (V), and V (V) and V (IV) (Casañ-pastor and Baker, 1992), exhibit significantly improved heat stability and acid–base stability compared with their prototype heteropoly acids. So far, little work has been focused on the anti-virus activity of these complexes.

In this paper, a series of novel heteropoly blues, $Ln_2H_3[BW_9{}^{VI}W_2{}^{V}Mn(H_2O)O_{39}]\cdot 12H_2O$ (Ln(2), Ln = La, Ce, Pr, Nd, Sm, Eu and Gd), have been synthesized and characterized, and their anti-virus activity against influenza virus in MDCK cells has been investigated. The results shown that these complexes exhibit anti-virus activities against influenza A and B comparable with that of virazole, and almost no cytotoxicity. Furthermore, the results also indicated that the anti-virus activities are in relation to the structure of these complex' anti-ion.

2. Materials and methods

2.1. Synthesis of $Ln_2H[BW_{11}Mn(H_2O)O_{39}]\cdot 12H_2O$

$K_9HBW_{11}O_{39}\cdot 13H_2O$ was synthesized according to the literature (Zhang et al., 1995).

$K_9HBW_{11}O_{39}\cdot 13H_2O$(19 g, 5 mmol) was added slowly to H_2O (80 ml) at 80 °C. The pH value of the solution was adjusted to 6.3 with HOAc–NaOAc–dioxane buffer, and then $Mn(NO_3)_2\cdot 6H_2O$ (1.72 g, 6 mmol) in H_2O (20 ml) was added slowly. The temperature was kept at 80 °C during the course. After 30 min, the pH value of the mixture was readjusted to 5.4, and rare earth carbonate (4 mmol) in H_2O (10 ml) was added drop-wise under stirring. The mixture was then stirred at 80 °C for 1 h, and the pH value was readjusted to 6.3. After filtering and cooling, the mixture was kept stirring for 2 h, and then kept at room temperature for several days. The crude products $Ln_2H[BW_{11}Mn(H_2O)O_{39}]\cdot 12H_2O$ abbreviated to Ln(0) (Ln = La, Ce, Pr, Nd, Sm and Gd) were obtained and re-crystallized in water.

2.2. Synthesis of $Ln_2H_3[BW^{VI}{}_9W^{V}{}_2Mn(H_2O)O_{39}]\cdot 12H_2O$

$Ln_2H[BW_{11}Mn(H_2O)O_{39}]\cdot 12H_2O$ (1.0 g) was dissolved in HOAc–NaOAc–dioxane buffer (50 ml, 0.1 mol dm^{-3}, pH = 5.4) and electrolytically under N_2 atmosphere at a controlled potential (ca. −0.545 V). The reduction process was monitored by polarography and UV spectra and the extent of reduction was checked by a copper coulometer. Then the reduced solution was transferred to a vacuum drier with silica gel and nitrogen atmosphere. After 7 days, the dark blue crystal $Ln_2H_3[BW^{VI}{}_9W^{V}{}_2Mn(H_2O)O_{39}]\cdot 12H_2O$ (Ln = La, Ce, Pr, Nd, Sm and Gd) abbreviated to Ln(2) were obtained and re-crystallized in water. Yields: 58.6–65.2%.

2.3. Cells and culture media

Madin–Darby canine kidney (MDCK) cells were obtained from the Chinese Academy of Military Medical Sciences (Peking, China). Typing culture collection, the MDCK cells were grown in Eagle's minimum essential medium (MEM) containing 5% fetal bovine serum (FBS, From Gibco). When used with influenza viruses, the MEM was supplemented with 10 U ml^{-1} of trypsin (Sigma), 1 μg ml^{-1} of EDTA, 0.18% $NaHCO_3$ and 50 μg ml^{-1} of gentamicin. Ninety six-well flat-bottomed microplates were used in vitro antiviral experiments and virus titrations.

2.4. Viruses and subculture

Influenza viruses (A/H1N1/Jingfang/1/91, A/H3N2/Jingfang/30/95 and B/Hufang/1/87) were obtained from the Chinese Academy of Medical Sciences (Peking, China). The virus was propagated for 3 days at 35 °C in chorio-allantoic cavities of 10-day-old embryonated hen eggs. The infected allantoic fluids were clarified by centrifugation at 1000 × *g* for 20 min and stored in small portions at −80 °C as the virus stock solution. The MDCK cells were cultured as monolayers in MEM supplemented with 8% fetal bovine serum.

2.5. In vitro antiviral assays

The in vitro antiviral activity of each complex was evaluated by the inhibition of visually discerned viral cytopathic effect (CPE) as literature (Huffman et al., 1997). The virus-induced cytopathogenic effect CPE was scored after 72 h under an inverted microscope (score 0 = 0% CPE, score 1 = 0–25% CPE, score 2 = 25–50% CPE, score 3 = 50–75% CPE and score 4 = 75–100% CPE). Confluent monolayers of MDCK cells in 96-well plates were rinsed once with MEM devoid of serum, the 100 $TCID_{50}$ ($TCID_{50}$: 50% tissue culture infective dose) virus was added to blotted plates followed by equal volumes of complexes at varying half-log 2 × concentrations in MEM. The wells devoid of drug were completely destroyed by virus after 3 days incubation at 37 °C.

Plates were read visually and then treated with stain. Cytotoxicity determinations were conducted by seeding MDCK cells into microplates at 4×10^3 cells per well. After an overnight incubation, complex in MEM containing 5% FBS was added. Cells were allowed to grow for an additional 3 days. Plates were read visually for toxicity and then treated with stain.

A 50% virus-inhibitory (effective) concentration (EC_{50}) was determined. The concentration required to cause a microscopically detectable alteration of normal cell morphol-

ogy was estimated as the minimum cytotoxic concentration (MCC), which was expressed as the 50% cell-inhibitory concentration (CC_{50}). The inhibition of MDCK cells growth was determined by the MTT method as described previously (Ferrari et al., 1990). Selectivity Indexes (SI) were determined as CC_{50} (resting cells)/EC_{50}. In general, the EC_{50} values using neutral red were two to five times higher than using visually discerned CPE, and the viral inhibition was determined at this dosage level.

2.6. Plaque reduction assay

Confluent monolayers in 5 cm dishes were inoculated with 100 PFU/0.5 ml of virus and washed twice with PBS after adsorption for 30 min, and then overlaid with drug-containing agarose. The monolayers were stained with 0.01% neutral red after 48 h at 37 °C and the plaques counted. The concentration reducing plaque number by 50% (EC_{50}) was evaluated (Serkedjeva and Hay, 1998).

3. Results

3.1. Redox properties

Complexes Ln(2) were prepared by electrolytically reducing the corresponding Ln(0) under controlled potential (ca. 4.5 V). The redox properties of Ln(0) and Ln(2) were investigated by cyclic voltammetric and polarographic methods. The CV diagram of Pr(2) was shown in Fig. 1. The half-wave potentials and CV data of Ln(0) and Ln(2) were listed in Table 1.

The CV diagram of Ln(0) exhibits two reversible redox peaks (Fig. 1), assigned to the reduction of two tungsten (VI) to (V). The number of electrons involved in the reduction process was calculated as two from the slopes of the straight lines obtained by logarithmic analysis in each of the two polarographic waves, indicating that each of the title complexes undergoes a two-step, two-electron reduction process. The half-wave potential of Ln(2) changed little with different rare earth ions (Table 1), indicating the rare earth ions do not take part in the redox process. In addition to the polarography of Ln(2) in the HOAc–NaOAc–dioxane buffer (pH = 6.3) exhibit two reduction waves with similar shape and height, indicating Ln(2) keep the Keggin structure as its prototype compound do.

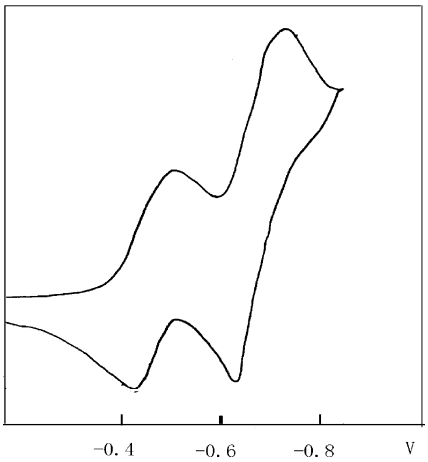

Fig. 1. Cyclic voltammograms of Pr(2) in the 0.5 M HOAc–NaOAc–dioxane buffer, pH 6.3, scan rate, 200 mV s^{-1}.

Table 1
Polarography and cyclic voltammetry data of heteropoly complexes

Complex	$E_{1/2}$ (V)		E_{pa} (V)	E_{pc} (V)	ΔE_p (mV)
La(0)	−0.438	−0.652	−0.432 −0.640	−0.498 −0.706	66 (66)
La(2)	−0.426	−0.641	−0.426 −0.648	−0.492 −0.715	66 (67)
Ce(0)	−0.436	−0.654	−0.431 −0.642	−0.498 −0.708	67 (66)
Ce(2)	−0.425	−0.639	−0.424 −0.650	−0.490 −0.716	66 (66)
Pr(0)	−0.439	−0.656	−0.430 −0.642	−0.495 −0.708	65 (66)
Pr(2)	−0.425	−0.639	−0.424 −0.649	−0.490 −0.716	66 (67)
Nd(0)	−0.432	−0.652	−0.430 −0.642	−0.496 −0.708	66 (66)
Nd(2)	−0.420	−0.631	−0.425 −0.646	−0.492 −0.71	67 (67)
Sm(0)	−0.441	−0.660	−0.431 −0.642	−0.498 −0.708	67 (66)
Sm(2)	−0.429	−0.642	−0.427 −0.647	−0.493 −0.714	66 (67)
Gd(0)	−0.442	−0.662	−0.430 −0.639	−0.497 −0.706	67 (66)
Gd(2)	−0.428	−0.644	−0.426 −0.648	−0.492 −0.715	66 (67)

3.2. IR spectra

The IR spectra of Ln(2) exhibit four characterized asymmetric stretching vibrations for heteropolyanions at 985, 943, 895 and 822 cm^{-1}, assigned to W = Od (Od, terminal oxygen), W–Ob–W (Ob, bridging oxygen), W–Oc–W (Oc, bridging oxygen atom) and B–Oa (Oa, central oxygen atom), respectively. The equivalent bands were observed for Ln(0) at 981, 938, 891 and 824 cm^{-1}, respectively. These data indicated that Ln(2) retain the Keggin structure of their prototype complexes but with slight distortion.

3.3. UV-Vis spectra

In the UV range, the electronic spectra of heteropoly acids Ln(0) exhibit two absorption at about 203 and 248 nm, which

Table 2
The inner electron binding energy data of the complexes

Complex	Ln ($3d_{5/2}$)	Mn ($2p_{3/2}$)	W ($4f_{7/2}$)	B ($2p_{1/2}$)	O (1s)
Ce(0)	886.5	641.7	36.1	192.8	532.9
Ce(2)	886.0	641.2	35.6	192.4	532.3
Pr(0)	933.1	641.6	36.1	192.6	532.2
Pr(2)	932.8	641.0	35.5	192.2	532.1

attributed to the transition of Od = W and Ob(Oc)–W, respectively. For heteropoly blues Ln(2) at the same conditions, the absorption ascribed to Od = W and Ob(Oc)–W was weakened, and shift to 193 ($\Delta\lambda = 10$ nm) and 239 nm ($\Delta\lambda = 10$ nm), respectively.

In the visible range, the electronic spectra of Ln(0) heteropolyanions exhibit an intense absorption at about 472 nm, ascribed to the d–d transition of Mn^{2+}. However, the spectra of heteropoly blues Ln(2) exhibit two intense absorption at about 720 and 472 nm, ascribed to the characterized B band. The absorption at 472 nm can be regarded as IVCT transition attributed to the charge-transfer between W(V) and W(VI) with Ob as bridging oxygen, according to the position and intensity (Casañ-pastor and Baker, 1992). The absorption at 472 nm indicates that Mn^{2+} is still present in the heteropoly blue and not affected by reduction.

3.4. Thermal gravimetric and differential thermal analysis

The decomposition temperatures for La(0) and La(2) are 345 and 378 °C, respectively. These data indicated that the heat stability of La(2) is higher than that of La(0) due to the increase of negative charge on the surface of anions. The TG curves of the heteropoly blues were composed of three lose weight steps. The DTA curves of heteropoly blues were composed of three endothermal peaks (corresponding to the loss of crystallization water, combined water and coordinated water) and one exothermal peak (corresponding to the loss of structure water and the decomposition of the complexes). The title complexes all show an endothermal process followed by an exothermal process, ascribed to the participation of water in coordination, marking the formation of 1:11 series complexes.

3.5. XPS spectra

The XPS spectra of La(0) and La(2) were measured and the inner electron binding energies were listed in Table 2, and the enlarged figure of $W4f_{5/2}$ and $W4f_{7/2}$ of Pr(2) were shown in Fig. 2.

The inner electron binding energy of W, Ln, O, B and Mn decreased in Ln(2) compared with the corresponding Ln(0) ascribed to the increase of charge density over the anions of Ln(2). These data also indicated that the extra electrons are, to a certain extent, delocalized in the whole molecule. The presence of Ln^{3+} and Mn^{2+} indicates that they are not affected during the reduction process. Compared with Ln(0),

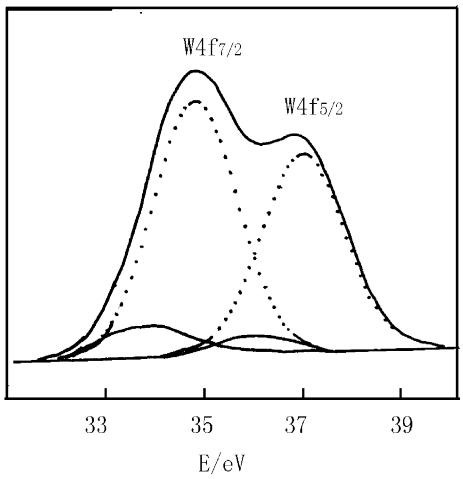

Fig. 2. XPS spectra of Pr(2).

the peak shape of the Ln(2) was broader and deformed. This may be attributed to the additive result of the splitting peaks for both W^{VI} and W^{V} upon the reduction process. When deconvoluted (Fig. 2), the area ratio of these peaks was 9:2, demonstrating that the reduced Ln(2) have two W^{V} atoms as expected.

3.6. The anti-influenza virus efficacy and cytotoxicity of heteropolymetalates by CPE

MDCK is sensitive to influenza virus (Margarita et al., 1997). In the absence of heteropolymetalates, small pathological change was observed for MDCK cells in microscope after 8 h infected by influenza virus A/N1H1/Jingfang/1/91, A/H3N2/Jingfang/30/95 or B/Hufang/1/87. The pathological changes reached to 80% 18 h later and 100% 72 h later. The pathological changes of MDCK in presence of heteropolymetalates were apparently at large dosage ($P < 0.05$), whereas almost the same at small dosage ($P > 0.05$). The experiment in vitro (at least once) showed that there were no cytotoxicity observed for Pr(2) in either resting or rapidly dividing cells at dosages as high as 256.8 μM.

The results of anti-influenza virus efficacy in MDCK cells by CPE methods were listed in Table 3. These results indicated that the controls $Mn(NO_3)_2{\cdot}6H_2O$ had no antiviral activity but obvious cytotoxicity, while $K_6H_3[BW_{11}MnH_2O]O_{39}]{\cdot}13H_2O$ had a little antiviral activity. All heteropolymetalates except Sm(0), Sm(2), Gd(0) and Gd(2) exhibit perfect antiviral activity against influenza A(A/N1H1/Jingfang/1/91, A/H3N2/Jingfang/30/95) compared to the control $Mn(NO_3)_2{\cdot}6H_2O$ and $K_6H_3[BW_{11}Mn(H_2O)O_{39}]{\cdot}13H_2O$. Meanwhile, all heteropolymetalates except Gd(0) and Gd(2) exhibit perfect antiviral activity against influenza B(B/Hufang/1/87) compared with the controls. Furthermore, $Ce_2H_3[BW_{11}Mn(H_2O)O_{39}]{\cdot}12H_2O$ showed the highest antiviral activity against influenza A (the EC_{50} was 1.8, 3.1 and 2.5 μM for A/N1H1/Jingfang/1/91, A/H3N2/Jingfang/30/95 and B/Hufang/1/87, respectively)

Table 3
The anti-influenza virus activity of complexes in MDCK cells

Complex	CC_{50} (μM)[a]	Virus					
		A/N1H1/Jingfang/1/91		A/H3N2/Jingfang/30/95		B/Hufang/1/87	
		EC_{50} (μM)[b,c]	SI[d]	EC_{50} (μM)	SI[d]	EC_{50} (μM)	SI[d]
La(0)	210.8	7.8	27.0	7.8	27.0	8.7	24.2
La(2)	243.2	5.6	43.4	6.8	35.7	7.7	31.5
Ce(0)	192.1	3.7	51.9	4.6	41.7	5.6	34.3
Ce(2)	241.5	1.8	134	3.1	78.1	2.5	96.8
Pr(0)	226.1	3.4	66.5	4.0	56.5	4.0	56.5
Pr(2)	256.8	2.5	102.8	3.7	69.4	2.2	116.8
Nd(0)	210.1	5.6	37.5	5.6	37.5	8.6	24.4
Nd(2)	242.4	4.9	49.4	4.9	49.4	7.7	31.4
Sm(0)	206.3	–[e]	–	–	–	9.8	21.0
Sm(2)	238.5	–	–	–	–	9.2	25.9
Eu(0)	206.1	4.9	42.0	5.2	39.6	5.5	37.4
Eu(2)	239.5	4.3	55.3	4.6	51.7	4.6	51.7
Gd(0)	233.0	–	–	–	–	–	–
Gd(2)	202.2	–	–	–	–	–	–
$Mn(NO_3)_2{\cdot}6H_2O$	836.1	–	–	–	–	–	–
$K_6H_3[BW_{11}Mn\ (H_2O)O_{39}]{\cdot}13H_2O$	174.9	70.8	2.67	64.0	2.95	67.4	2.8
Virazole	5755.6	53.2	108.2	53.2	108.2	69.6	82.6

[a] 50% cell toxicity concentration determined by MTT assay.
[b] Mean of CPE inhibition and NR uptake data.
[c] Concentration reducing by 50% the optical density values (or the virus-induced CPE in PC-treated virus-infected cells in relation to virus control). The value of EC_{50} is the mean of three experiments.
[d] Selectivity Index (CC_{50}/EC_{50}).
[e] Lower than 50% inhibitory cytopathic induced by virus.

Table 4
Anti-influenza virus activity of complexes in MDCK cells by PFU method[a]

Complex	Virus					
	A/N1H1/Jingfang/1/91		A/H3N2/Jingfang/30/95		B/Hufang/1/87	
	EC_{50} (μM)[b]	Si[c]	EC_{50} (μM)	SI	EC_{50} (μM)	SI
La(0)	8.7	24.2	9.0	23.4	8.1	26.0
La(2)	7.1	34.2	7.4	32.8	6.8	35.7
Ce(0)	3.1	61.9	3.7	51.9	2.5	76.8
Ce(2)	2.5	96.8	3.7	65.4	2.2	110.0
Pr(0)	3.7	61.1	4.0	56.5	3.7	61.1
Pr(2)	2.5	102.8	3.7	69.4	2.2	116.8
Nd(0)	6.2	33.9	5.6	37.5	7.7	27.3
Nd(2)	4.9	49.4	4.9	49.4	6.5	37.3
Sm(0)	–[d]	–	–	–	9.2	22.4
Sm(2)	–	–	–	–	9.2	25.9
Eu(0)	–	–	5.2	39.6	5.5	37.4
Eu(2)	4.3	55.3	4.6	51.7	4.6	51.7
Gd(0)	–	–	–	–	–	–
Gd(2)	–	–	–	–	–	–
$Mn(NO_3)_2{\cdot}6H_2O$	–	–	–	–	–	–
$K_6H_3[BW_{11}Mn(H_2O)O_{39}]{\cdot}13H_2O$	64.0	2.7	60.9	2.9	62.5	2.8
Virazole	49.2	117.0	53.2	108.2	65.5	87.9

[a] The experiments were done in duplicate as described in Section 3.7. The results are presented as a percentage of virus control and are the mean values form three independent experiments minute plaques were observed.
[b] 50% virus-inhibitory (effective) concentration.
[c] Selectivity Index (CC_{50}/EC_{50}).
[d] Lower than 50% inhibitory cytopathic induced by virus.

and $Pr_2H_3[BW_{11}Mn(H_2O)O_{39}]\cdot 12H_2O$ showed the highest antiviral activity against influenza viruses B (EC_{50} = 2.2 μM).

3.7. Anti-influenza virus efficacy of complexes by PFU methods

The anti-influenza virus activities of these heteropolymetalates in MDCK cells have also been studied by PFU method (Table 4). A complex was considered as inhibiting virus if plaques do not or seldom occur in the groups with the complex added in, while the plaques occur in the control groups. The EC_{50} for Ce(2) against influenza A/N1H1/Jingfang/1/91, A/H3N2/Jingfang/30/95 and B/Hufang/1/87 was 2.5, 3.7 and 2.2 μM, respectively. The EC_{50} for Pr(2) against influenza A/N1H1/Jingfang/1/91, A/H3N2/Jingfang/30/95 and B/Hufang/1/87 at the same condition was 2.5, 3.7 and 2.2 μM, respectively. These data are in agreement with that of CPE, implying Pr(2) and Ce(2) exhibit the highest inhibitory activity against influenza A and B.

4. Discussion

In this paper, a series of novel heteropoly blues, $Ln_2H_3[BW_9{}^{VI}W_2{}^{V}Mn(H_2O)O_{39}]\cdot 12H_2O$ (Ln = La, Ce, Pr, Nd, Sm, Eu and Gd), as well as their prototype heteropoly acids, have been prepared and characterized by elemental analysis, IR, UV, CV, TG-DTA, XPS and electrochemistry. The results shown that heteropoly blues (Ln(2)) keep α-Keggin structure but with a subtle distortion compared with their corresponding heteropoly acid (Ln(0)) do. The study by TG-DTA also indicated that the heat stability of Ln(2) is higher than the corresponding Ln(0).

The antiviral activity of Ln(2), as well as the corresponding Ln(0), against influenza A and B virus have been investigated by CPE and plaque reduction assay. Although all of these complexes exhibit a similar inhibitory activity against influenza virus, the sensitivity varied appreciably. The results also show that Ce(2) exhibit the highest inhibit activity against influenza virus A and Pr(2) exhibit the highest inhibit activity against influenza virus B. On the contrary, the heteropolyoxometalates containing Eu showed almost no antiviral activity against both influenza virus A and B. This may explained with that heteropoly blues containing Ce(2) or Pr(2) have a suitable molecular size to interfere and destroy the virus or virus' chemical components. Furthermore, from Tables 3 and 4, it's shown that the antiviral activity of these heteropolyoxometalates were determined by their anionic structures (Ikeda et al., 1994; Ni et al., 1994, 1996), the peripheral rare earth ions (Inouye et al., 1992, 1993), the substituted metal ions and the number of the anionic negative charges (Ikeda et al., 1993; Mori et al., 1995).

The antiviral activity of Ln(2) was superior to that of their parent heteropoly acids, and the cytotoxicity was inferior (Table 3). This may be attributed to the lower heat stability of Ln(0) compared to Ln(2), resulting in a relatively large concentrations of rare earth ions Ln^{3+} and $WO_4{}^{2-}$ released by the decomposing of Ln(0) within a short period, and the concentrations of rare earth ion Ln^{3+} and $WO_4{}^{2-}$ is high enough to exhibit high cytotoxicity (Teruaki et al., 1990). On the contrary, heteropoly blues decompose more slowly and the concentrations of metal ions dissociated are moderate due to their higher heat stability.

Acknowledgements

This work was supported by the Guangdong Natural Science Foundation (No. 031580) and Guangdong Science technology plant item (No. 2003C30103).

References

Bardos, T.J., Schinazi, R.F., Ling, K.H.J., Heider, A.R., 1992. Structure activity relationship and mode of action of 5-mercapto-substituted oligo- and polynucleotides as antitemplates inhibiting replication of human immunodeficiency virus type 1. Antimicrob. Agents Chemother. 36, 108–114.

Barnard, D.L., Hill, C.L., Gage, T., Matheson, J.E., Huffman, J.H., Sidwell, R.W., Otto, M.I., Schinazi, R.F., 1997. Potent inhibition of respiratoy syncytial virus by polyoxometalates of several structural classes. Antiviral Res. 34, 27–37.

Burger, R.A., Billingsley, J.L., Huffman, J.H., Bailey, K.W., Kim, C.U., 2000. Immunological effects of the orally administered neuraminidase inhibitor oseltamivir in influenza virus-infected and uninfected mice. Immunopharmacology 47, 45–52.

Busserearu, F., Picard, M., Blancou, J., Sureau, P., 1988. Treatment of rabies in mice and foxes with antiviral compounds. Acta Virol. 32, 33–49.

Casañ-pastor, N., Baker, L.C.W., 1992. Magnetic properties of mixed-valence heteropoly blues. J. Am. Chem. Soc. 114, 10384–10394.

Colman, P.M., 2002. Neuraminidase inhibitors as antivirals. Vaccine 20, S55–S58.

Dan, K., Miyashita, K., Seto, Y., Fujita, H., Yamase, T., 2002. The memory effect of heteropolyoxotungstate (PM-19) pretreatment on infection by herpes simplex virus at the penetration stage. Pharm. Res. 46, 357–362.

Ferrari, M., Chiara, M., Isetta, A.M., 1990. MTT colorimetric assay for testing macrophage cytotoxic. J. Immunol. Methods 131, 165–172.

Fukuma, M., Seto, Y., Yamase, T., 1991. In vitro antiviral activity of polyoxotungstate (PM-19) and other polyoxometalates against herpes simplex virus. Antiviral Res. 16, 327–339.

George, C.X., Singh, C., Ram, S.N., Yadav, K.D.S., Sharma, B., 1990. Studies on the antiviral activity of inorganic heteropolyanions against semliki forest virus in vivo and vaccinia virus in vitro. Acta Virol. 34, 330–338.

Heider, H., Adamczyk, B., Presber, H.W., Schroeder, C., Feldblum, R., Indulen, M.K., 1981. Occurrence of amantadine and rimantadine resistant influenza A virus strains during the epidemic. Acta Virol. 25, 395–400.

Hill, C.L., Weeks, M.S., Schinazi, R.F., 1990. Anti-HIV activity, toxicity, and stability studies of representative structural families of polyoxometalates. J. Med. Chem. 33, 2767–2772.

Huffman, J.H., Sidwell, R.W., Barnard, D.L., Morrison, A., Otto, M.J., Hill, C.L., Schinazi, R.F., 1997. Influenza virus-inhibitory effects of a series of germanium and silicon-centered polyoxometalates. Antiviral Chem. Chemother. 8, 75–83.

Ikeda, S., Nishiya, S., Yamamoto, A., Yamaser, T., Nishimura, C., De Clercq, E., 1993. Activity of the Keggin polyoxotungstate PM-19 against herpes simplex virus type 2 infection in immunosuppressed mice: role of peritoneal macrophage activation. J. Med. Virol. 41, 191–195.

Ikeda, S., Nishiya, S., Yamamoto, A., Yamase, T., Nishimura, C., De Clercq, E., 1994. Antiviral activity of a Keggin Polyoxotungstate PM-19 against herpes simplex virus in mice. Antiviral Chem. Chemother. 5 (1), 47–50.

Ikeda, S., Neyts, J., Yamamoto, N., Murrer, B., Theobald, B., Bossard, G., Henson, G., Abrams, M., Picker, D., De Clercp, E., 1993. In vitro activity of a novel series of polyoxosilicotungstates against human myxo-, herpes- and retroviruses. Antiviral Chem. Chemother. 4 (5), 253–262.

Inouye, Y., Tokutake, Y., Kunihara, J., Yoshida, T., Yamase, T., Nakata, A., Nakamura, S., 1992. Suppressive effect of polyoxometalates on the cytopathogenicity of human immunodeficiency virus type 1 (HIV-1) in vitro and their activity against HIV-1 Reverse transcriptase. Chem. Pharm. Bull. 40 (3), 805–807.

Inouye, Y., Take, Y., Tokutake, Y., Yoshida, T., Yamamoto, A., Yamase, T., Nakamura, S., 1990. Inhibition of replication of human immunodeficiency virus by a heteropolyoxotungstate (PM-19). Chem. Pharm. Bull. 38 (1), 285–287.

Inouye, Y., Tokutake, Y., Yoshida, T., Yamamoto, A., Yamase, T., Nakamura, S., 1991. Antiviral activity of polyoxomolybdoeuropate PM-104 against human immunodeficiency virus type 1. Chem. Pharm. Bull. 39 (6), 1638–1640.

Inouye, Y., Tokutake, Y., Yoshida, T., Seto, Y., Hujita, H., Dan, K., Yamamoto, A., Nishiya, S., Yamase, Y., Nakamura, S., 1993. In vitro antiviral activity of polyoxomolybdates. Mechanism of inhibitory effect of PM-104 $(NH_4)_{12}H_2(Eu_4(MoO_4)H_2O_{16}(Mo_7O_{24})_4)\cdot 13H_2O$ on human immunodeficiency virus type 1. Antiviral Res. 20, 317–331.

McKimm-Breschkin, J.L., 2000. Resistance of influenza viruses to neuraminidase inhibitors—a review. Antiviral Res. 47, 1–17.

Jeffrey, T., Hill, C.L., Judd, D.A., 1998. Polyoxometalates in medicine. Chem. Res. 98, 327–357.

Kim, G.S., Judd, D.A., Hill, C.L., Schinazi, R.F., 1994. Synthesis, characterization, and biological activity of a new potent class of anti-HIV agents, the peroxoniobium-substituted heteropolytungstates. J. Med. Chem. 37, 816–820.

Liu, J., Wang, E.B., Zhou, Y.S., Peng, J., 1998a. Studies on anti-influenza virus activity of heteropoly complexes containing rare earth elements. J. Chin. Rare Earth Soc. 16 (3), 257–261.

Liu, J., Wang, E.B., Wang, Z.P., Hu, C.W., 1998b. Synthesis and properties of rare earth molybdosilicic heteropoly blues substituted by cobalt. Chem. J. Chin. Univ. 19, 1200–1204.

Liu, J., Mei, W.J., Li, Y.G., Wang, E.B., Ji, L.N., Tao, P.Zh., 2000. Antiviral activity of mixed-valence rare earth borotungstate heteropoly blues against influenza virus in mice. Antiviral Chem. Chemother. 11, 367–372.

Margarita, D.G., Carmen, R., Mariano, E., 1997. Activation of the IFN-inducible enzyme Rnase L causes apoptosis of animal cells. Virology 236, 354–363.

Mori, S., Watanabe, J., Shigeta, S., 1996. Dramatic combination therapy with Ribavirin and Polyoxometalate in the treatment of Influenza A virus infected mice. Antiviral Res. 30, A53.

Mori, S., Watanabe, J., Baba, M., Khenkin, A.M., Hill, C.L., Schinazi, R.F., 1995. In vitro antimyxovirus and anti-human immunodeficiency virus activities of polyoxo-metalates. Antiviral Chem. Chemother. 6, 114–122.

Moskovitz, B.L., 1988. Clinical trial of tolerance of HPA-23 in patients with acquired immune deficiency syndrome. Antimicrob. Agents Chemother. 32 (9), 1300–1303.

Ni, L., Boudinot, F.D., Boudinot, S.G., Henson, G.W., Bossard, G.E., Martellucci, S.A., Ash, P.W., Fricker, S.P., Darkes, M.C., Theobald, B.R.C., Hill, C.L., Schinazi, R.F., 1994. Pharmacokinetics of antiviral polyoxometalates in rats. Antimicrob. Agents Chemother. 38, 504–510.

Ni, L., Greenspan, P., Gutman, R., Kelloes, C., Farmer, M.A., Boudinot, F.D., 1996. Cellular localization of antiviral polyoxometalates in J774 macrophages. Antiviral Res. 32, 141–148.

Ni, L., Boudinot, F.D., 1995. Non-linear renal and biliary clearances of antiviral Polyoxometalates in rats. Eur. J. Drug Metab. Pharmacokinet. 20, 209–217.

Pauwele, R., Balzarini, J., Baba, M., Snoeck, R., Schols, D., Herdewijn, P., Desmyter, J., De Clercq, E., 1988. Rapid and automated tetrazolium-based colorimetric assay for the detection of anti-HIV compounds. J. Virol. Methods 20, 309–321.

Serkedjeva, J., Hay, A.J., 1998. In vitro anti-influenza virus activity of a plant preparation from *Geranium sanguineum* L. Antiviral Res. 37, 121–130.

Shigeta, S., Mori, S., Watanabe, J., Yamasi, T., Hill, C.L., Schinazi, R.F., 1995a. Anti-influenza activities of polyoxometalates. Antiviral Res. 26, A298.

Shigeta, S., Mori, S., Watanabe, J., 1995b. In vitro antimyxovirus and anti-human immunodeficiency virus activities of polyoxometalates. Antiviral Chem. Chemother. 6, 114–122.

Sidwell, R.W., Huffman, J.H., Barnard, D.L., Bailey, K.W., Wong, M.H., Morrison, A., Syndergaard, T., Kim, C.U., 1998. Inhibition of influenza virus infections in mice by GS4104, an orally effective influenza virus neuraminidase inhibitor. Antiviral Res. 37, 107–120.

Take, Y., Tokutake, Y., Inouye, Y., Yoshida, T., Yamamoto, A., Yamase, T., Nakamura, S., 1991. Inhibition of proliferation of human immunodeficiency virus type1 by novel heteropolyoxotungstates in vitro. Antiviral Res. 15, 113–124.

Teruaki, H., Yuji, F., Yoshio, L., 1990. An in vitro chemosensitivity test for the screening of anti-cancer drugs in childhood leukemia. Cancer 65, 1263–1270.

Tomita, K., Yamase, T., Shishido, K., 1989. Medical chemistry of polyoxometalates. Inorg. Chim. Acta 157, 167–169.

Weeks, M.S., Hill, C.L., Schinazi, R.F., 1992. Synthesis, characterization and anti-human immunodeficiency virus activity of water soluble salts of Polyoxotungstate anions with covalently attached organic groups. J. Med. Chem. 35, 1216–1221.

Wilson, S.Z., Knight, V., Wyde, P.R., Drake, S., Couch, R.B., 1980. Amantadine and ribavirin aerosol treatment of influenza A and B infection in mice. Antimicrob. Agents Chemother. 17, 642–648.

Wray, S.K., Gilbert, B.E., Knight, V., 1985. Effect of ribavirin triphosphate on primer generation and elongation during influenza virus transcription in vitro. Antiviral Res. 5, 39–48.

Wray, S.K., Smith, R.H.A., Gilbert, B.E., Knight, V., 1986. Effects of selenazofurin and ribavirin and their 5′-triphosphates on replicative functions of influenza A and B viruses. Antimicrob. Agents Chemother. 29, 67–72.

Wyde, P.R., Wilson, S.Z., Gilbert, B.E., Smith, R.H.A., 1986. Protection of mice from lethal influenza virus infection with high dose-short duration ribavrin aerosol. Antimicrob. Agents Chemother. 30, 942–944.

Yamase, T., Fukuda, N., Tajima, Y., 1996. Synergistic effect of polyoxotyungstates in combination with β-lactam antibiotics on antibacterial activity against methicillin-resistant staphylococcus aureus. Biol. Pharm. Bull. 19 (3), 459–465.

Yamamoto, A., Schols, N.D., De Clercq, E., 1992. Mechanism of anti-human immunodeficiency virus action of polyoxometalates. A class of broad-spectrum antiviral agents. Mol. Pharmacol. 42, 1109–1117.

Zhang, X.Y., Pope, M.T., Chance, M.R., Jameson, G.B., 1995. High-valent manganese in polyoxotungstates manganese (IV) Keggin derivatives. Polyhedron 14, 1381–1392.